



Provenance of the Lower Triassic Clastic Rocks in the Southwestern Margin of the South China Craton and Its Implications for the Subduction Polarity of the Paleo-Tethyan Ocean

Chao Han^{1,2}, Hu Huang^{1,2*}, Chenchen Yang^{1,2}, Linxi Wang^{1,2} and Hongwei Luo^{1,2}

¹State Key Laboratory of Oil and Gas Reservoir Geology and Exploitation, Institute of Sedimentary Geology, Chengdu University of Technology, Chengdu, China, ²Key Laboratory of Deep-Time Geography and Environment Reconstruction and Applications of Ministry of Natural Resources, Chengdu University of Technology, Chengdu, China

OPEN ACCESS

Edited by:

Shengyao Yu,
Ocean University of China, China

Reviewed by:

Wenchao Yu,
China University of Geosciences
Wuhan, China

Bin Liu,
Yangtze University, China

*Correspondence:

Hu Huang
118huanghu@163.com

Specialty section:

This article was submitted to
Geochemistry,
a section of the journal
Frontiers in Earth Science

Received: 29 April 2022

Accepted: 23 May 2022

Published: 30 June 2022

Citation:

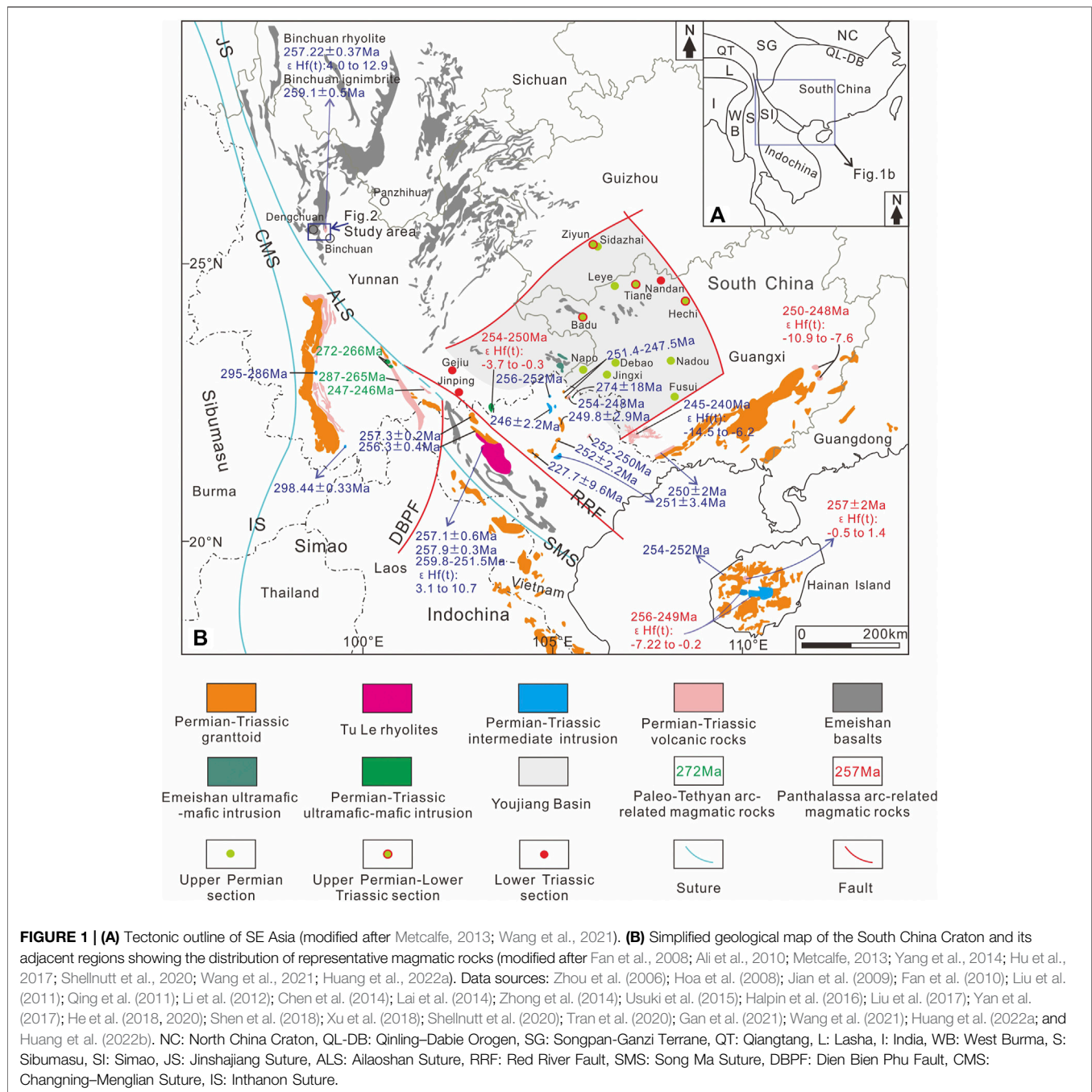
Han C, Huang H, Yang C, Wang L and Luo H (2022) Provenance of the Lower Triassic Clastic Rocks in the Southwestern Margin of the South China Craton and Its Implications for the Subduction Polarity of the Paleo-Tethyan Ocean.
Front. Earth Sci. 10:932486.
doi: 10.3389/feart.2022.932486

The southwestern margin of the South China Craton preserves a Late Permian to Early Triassic sedimentary succession, the provenance of which helps to constrain the magmatic history and tectonic evolution of the Paleo-Tethyan Orogen. In this study, we present new detrital zircon U-Pb age, trace element, Hf isotope and whole-rock geochemical composition analyses from the Lower Triassic Qingtianbao Formation, to distinguish the provenance of clastic rocks. The results show that the detrital zircons of the Qingtianbao Formation are characterized by an age spectrum of unimodal, with an age peak of ~260 Ma, and have a geochemical affinity to within-plate sources. Most of these zircons have positive $\epsilon_{\text{Hf}}(t)$ values (+1.6 to +5.9), similar to those of the Emeishan rhyolites. The whole-rock geochemistry of most clastic samples shows no Nb-Ta anomalies on primitive mantle-normalized elemental diagrams. These features imply a source related to the Emeishan volcanic rocks. Integration of the geologic and provenance records in the southwestern margin of the South China Craton, we suggest that the Paleo-Tethyan Ocean may undergo a unidirectional subduction westward beneath the Indochina Block during the Late Permian–Early Triassic.

Keywords: provenance, subduction polarity, Lower Triassic, South China Craton, detrital zircon, Paleo-Tethyan

1 INTRODUCTION

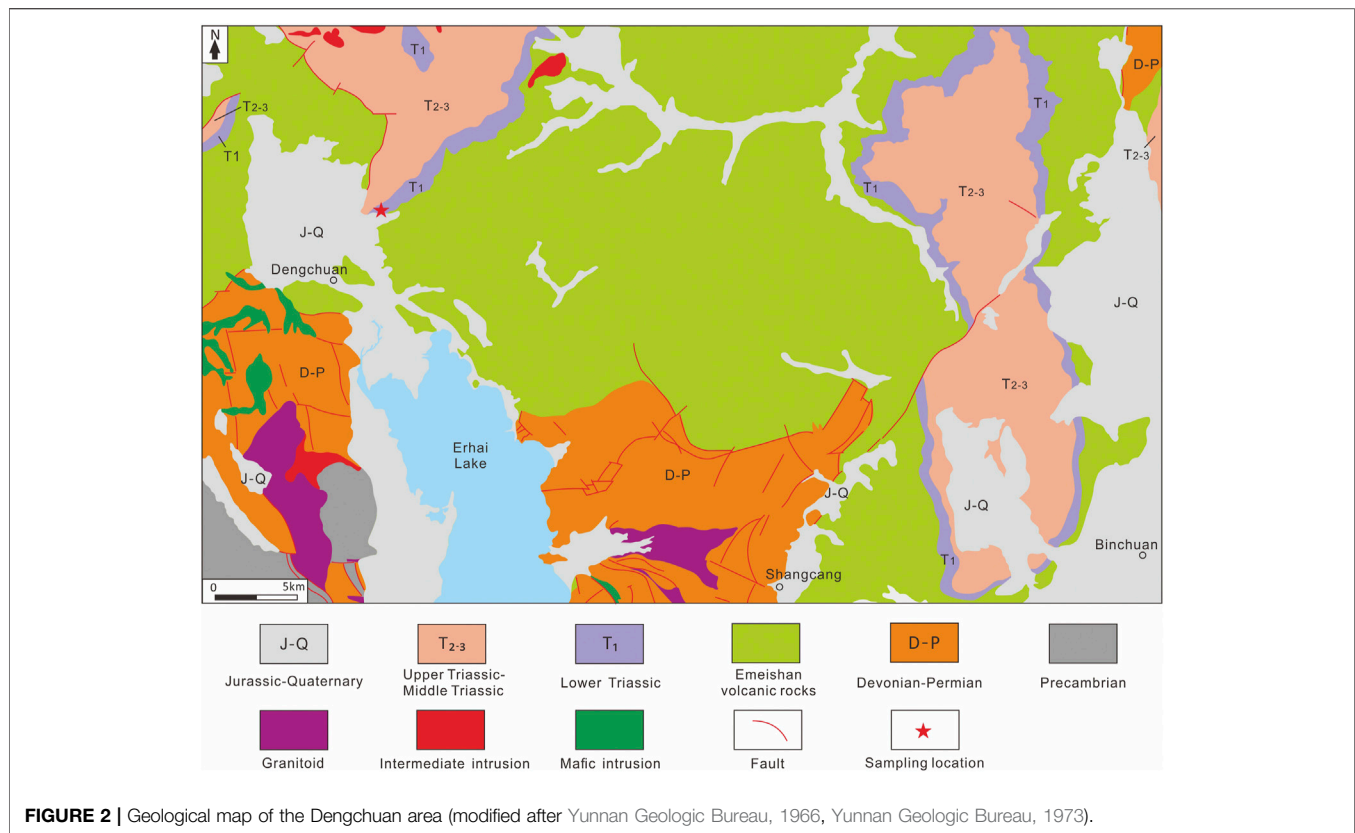
During the middle-late Paleozoic, the South China Craton separated from the Gondwana Land and then experienced convergence and collision, as well as accretion (Metcalf, 2013; Cawood et al., 2018; Wang et al., 2021). It made the Paleo-Tethyan Ocean gradually opened and closed during the Silurian–Triassic (Metcalf, 2006, 2013; Wang et al., 2021). Meanwhile, there are multiple tectonomagmatic events in the southwestern margin of the South China Craton and Indochina Block, including the Emeishan large igneous province (ELIP) (Figure 1) (Chung and Jahn, 1995; Xu et al., 2001, 2004, 2008; Xiao et al., 2004; Zhou et al., 2006; Huang et al., 2018). These magmatic rocks provide significant detritus for adjacent basins, which could reveal the tectonic setting of the basin (Cawood et al., 2012). Moreover, large volumes of magma are produced in the convergent plate margin settings, but rocks from this setting have comparatively poor potential for preservation in the geological record (Scholl and von Huene, 2009; Cawood et al., 2012). Magmatic rocks are poorly



exposed along the Paleo-Tethyan Ocean between the South China Craton and Indochina Block (**Figure 1**), and thus its subduction polarity has been controversial. Some studies suggested that the subduction was bidirectional (e.g., Zhong et al., 2013; Hou et al., 2017; Xia et al., 2019; Xu et al., 2019), whereas other studies argued that the subduction was unidirectional (e.g., Faure et al., 2014; Ngo et al., 2016; Yu et al., 2016; Gan et al., 2021; Li et al., 2021; Wang et al., 2021). The latter suggested that the southwestern margin of the South China Craton was a passive continental margin (Yan et al., 2019), and the Paleo-Tethyan Ocean may only undergo a subduction westward beneath the

Indochina Block during the Late Permian–Early Triassic (Jian et al., 2009; Faure et al., 2014; Ngo et al., 2016; Li et al., 2021; Wang et al., 2021).

In this study, we integrate new whole-rock geochemistry compositions, detrital zircon geochronological and geochemical data, as well as zircon Hf isotopic analyses of the Lower Triassic clastic rocks in the southwestern margin of the South China Craton. These data, when combined with data from the Late Permian to Early Triassic sequences in the southwestern South China Craton, allow us to better constrain the subduction polarity of the Paleo-Tethyan Ocean.



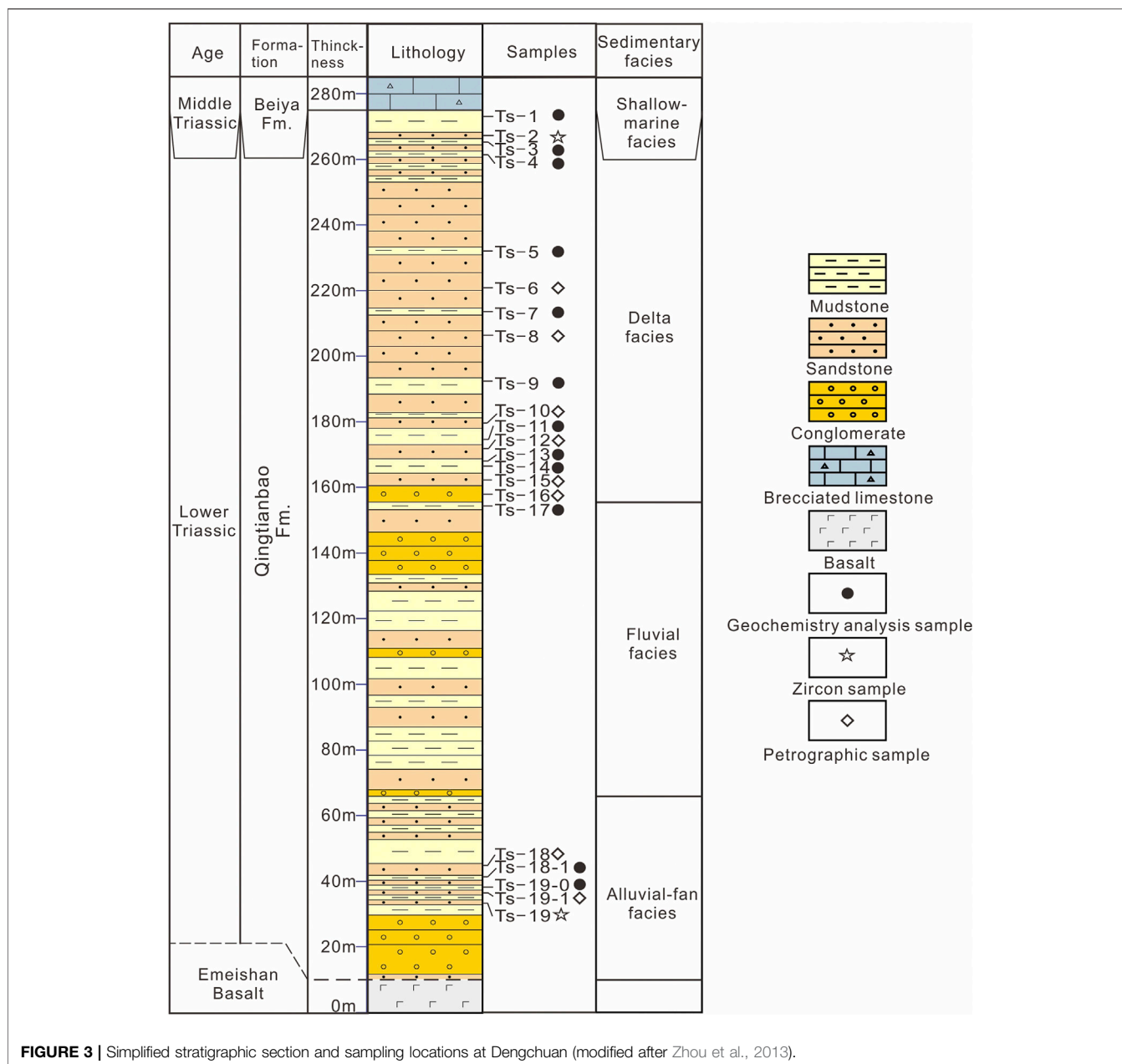
2 GEOLOGICAL SETTING

The South China Craton is bounded to the north by the Qinling–Dabie Orogen belt, to the northwest by the Songpan–Ganzi Terrane, and to the southwest by the Jinshajiang and Ailaoshan–Song Ma Suture (**Figure 1**) (Metcalf, 2013; Wang et al., 2021). It is adjacent to the Pacific Ocean to the southeast, and the rocks of Hainan Island are also considered to belong to it (Cawood et al., 2018). During the early Neoproterozoic, the South China Craton was formed by collision of the Yangtze and Cathaysia blocks (Li et al., 2009; Cawood et al., 2018). The Ailaoshan–Song Ma Suture between South China and Indochina/Siniao is known as the remnants of a branch of the Paleo-Tethyan Ocean (**Figure 1**) (Faure et al., 2014; Wang et al., 2021). This Paleo-Tethyan branch ocean is generally suggested to be opened in the Silurian–Devonian and finally closed no earlier than Middle Triassic (e.g., Jian et al., 2009; Fan et al., 2010; Zi et al., 2012; Xu et al., 2019). Opening and spreading of the Paleo-Tethyan branch ocean, expressed as transgression, led to regional subsidence in the western margin of the South China Craton and the deposition of the carbonate platform before the Middle Permian (Liu and Xu, 1994). During the late Middle Permian, the regional crustal uplift, called the “Dongwu uplift movement,” existed in the South China Craton and resulted in a widespread unconformity across most of South China (Hou et al., 2020). The ELIP was recognized as an important magmatic event that occurred in the South China Craton (Xu et al., 2001; Zhou et al., 2002; Xiao et al., 2004; Huang et al., 2014, 2016, 2018; Shellnutt et al., 2020). It mainly comprises voluminous continental flood basalt,

ultramafic–mafic intrusive and extrusive rocks, rhyolite, and granitic rock (Xu et al., 2001, 2010; Xiao et al., 2004; Zhou et al., 2006; Liu et al., 2016; Huang et al., 2022a). The ELIP mainly erupted around the Permian Guadalupian–Lopingian boundary (~260–257 Ma) (Zhou et al., 2002; Shellnutt et al., 2012, 2020; Zhong et al., 2014, 2020; Huang et al., 2016, 2018, 2022b). The eruption of the ELIP covers an area of $\sim 2.5 \times 10^5 \text{ km}^2$ in the South China and northern Vietnam (**Figure 1**) (Chung and Jahn, 1995; Xu et al., 2001; Ali et al., 2010), and its volume is $\sim 3.8 \times 10^6 \text{ km}^3$ (He et al., 2007). The total thickness of the volcanic sequence ranges from more than 5 km in the west of the province to several hundred meters in the east (He et al., 2007). The Emeishan volcanic rocks overlie the limestone-dominated Middle Permian Maokou Formation and are, in turn, covered by Upper Permian clastic rocks in the east and Lower Triassic sedimentary rocks in the west (He et al., 2007). The Emeishan basalts were often divided into high-Ti and low-Ti groups according to Ti/Y ratios and TiO_2 values (Xu et al., 2001). In the western parts of the ELIP, such as the Binchuan and Panzhihua areas (**Figures 1, 2**), the volcanic sequence is usually composed of low-Ti basalts at the bottom, high-Ti basalts in the middle, and felsic volcanic rocks (rhyolite and trachyte) at the top (Xu et al., 2010; Huang et al., 2022a).

3 SAMPLED STRATIGRAPHY AND ANALYTICAL METHODS

The Lower Triassic Qingtianbao Formation at Dengchuan consists of yellowish gray to purplish red sandstone,



mudstone, and conglomerate (**Figure 3; Figures 4A, B**). It is unconformably underlain by the Emeishan basalts and conformably overlain by breccia limestones of the Middle Triassic Beiya Formation (**Figure 3**) (Yunnan Geologic Bureau, 1973; Zhou et al., 2013). The Qingtianbao Formation can be classified into three sedimentary facies including alluvial-fan facies, fluvial facies, and delta facies (**Figure 3**) (Zhou et al., 2013). The vertical changes of sedimentary facies at Dengchuan indicate that the large-scale transgression occurred in this area, and it has experienced environmental changes from land to shallow sea during the Early Triassic to Middle Triassic (Zhou et al., 2013). Twenty-four samples, including ten petrologic samples, twelve geochemical analysis samples, and two zircon

analysis samples, were collected from the Qingtianbao Formation at Dengchuan, Yunnan Province, in the southwestern margin of the South China Craton (**Figures 2, 3**). The detrital compositions of sandstones from the Lower Triassic Qingtianbao Formation mainly comprise quartz (15–25%), feldspar (45–55%), and lithic fragments (15–45%). The dominant lithic fragments are basalts and felsic volcanic rocks (**Figures 4C, D**). Accessory minerals include zircon and magnetite. Both the roundness and sorting of sandstone samples are moderate (**Figures 4C, D**).

All samples were crushed (to 60 mesh) in a corundum jaw crusher. About 50 g of each sample was ground to a powder of less than 200 mesh in an agate ring mill. Whole-rock major and trace elements were analyzed with XRF (Primus II, Rigaku, Japan) and

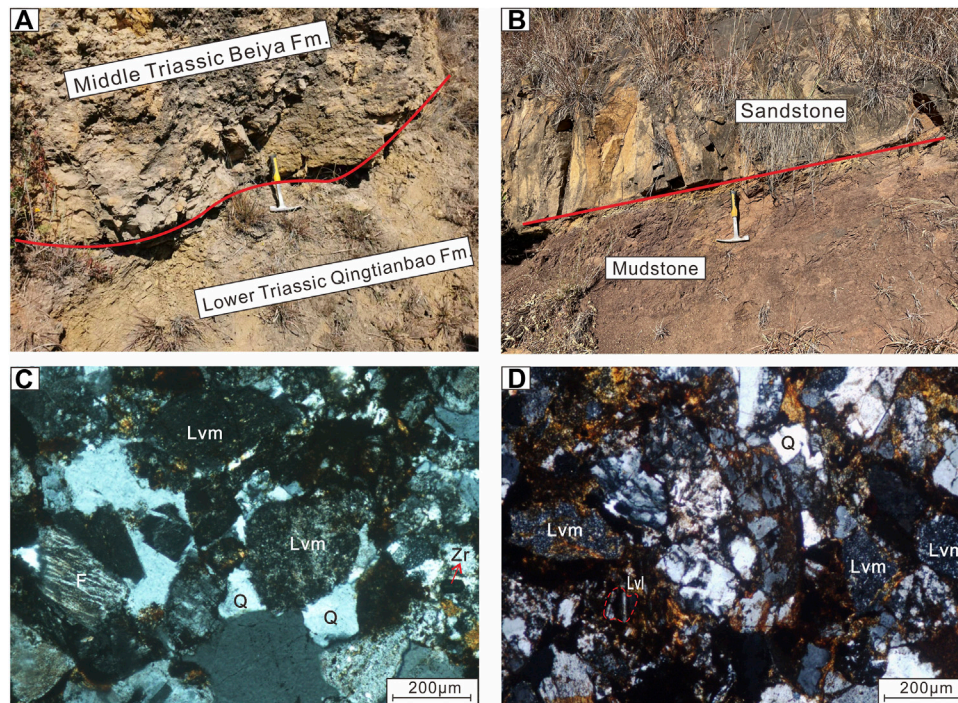


FIGURE 4 | Representative field outcrops and photomicrographs of clastic rocks at Dengchuan. **(A)** Boundary between the Middle Triassic Beiya Formation and Lower Triassic Qingtianbao Formation. **(B)** Sandstone and purple mudstone in the middle part of the Qingtianbao Formation. **(C)** Sandstone sample Ts-10. **(D)** Sandstone sample Ts-19. The photomicrographs of samples are in cross-polarized light. Volcanic rock fragments of lathwork (Lvl) and microlitic (Lvm); quartz (Q); feldspar (F); and zircon (Zr).

ICP-MS (Agilent 7700e) at Wuhan Sample Solution Analytical Technology Co., Ltd., Wuhan, China, respectively. The analytical precision is generally less than 5% and accuracy is better than 5% for most major and trace elements. The detailed analytical techniques of XRF and ICP-MS for element concentrations are the same as described by Ma et al. (2012) and Liu et al. (2008), respectively.

Zircon grains were separated by conventional heavy liquid and magnetic techniques, followed by hand picking under a binocular microscope and mounting in epoxy and polishing for the back-scattered electron (BSE) and cathodoluminescence (CL) imaging. U-Pb dating and trace element analysis of zircons were conducted by LA-ICP-MS at Wuhan Sample Solution Analytical Technology Co., Ltd., Wuhan, China. Detailed equipment configuration and data

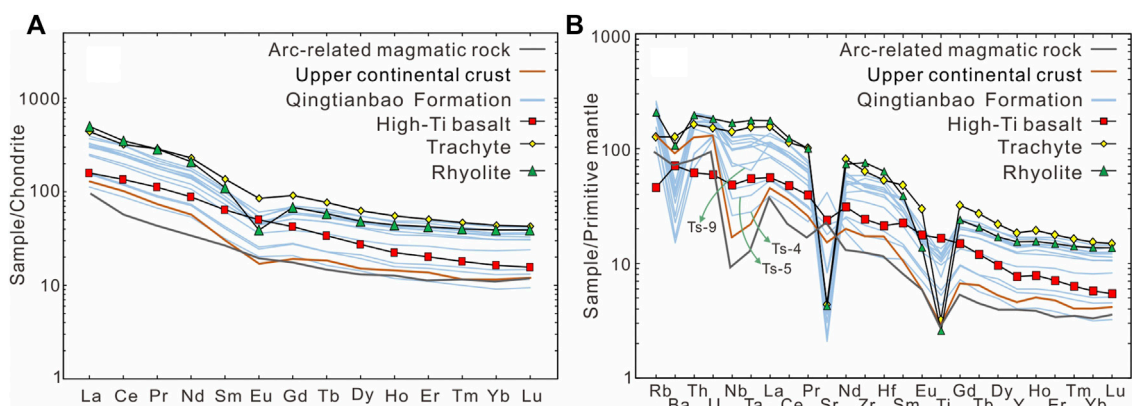


FIGURE 5 | (A) Chondrite-normalized REE diagram. **(B)** Primitive mantle-normalized trace element diagram. Normalized data are from Sun et al. (1989). The average upper continental crust (UCC) (Rudnick and Gao, 2003), arc-related magmatic rocks (Omrani et al., 2008), Emeishan high-Ti basalts (Xiao et al., 2003, 2004; Fan et al., 2008; Song et al., 2008; Anh et al., 2011; Lai et al., 2012; Huang et al., 2014), Emeishan rhyolites (Xu et al., 2010; Cheng et al., 2017; Hei et al., 2018; Huang et al., 2022a), and Emeishan trachytes (Shellnutt and Jahn, 2010; Xu et al., 2010) are displayed for comparison.

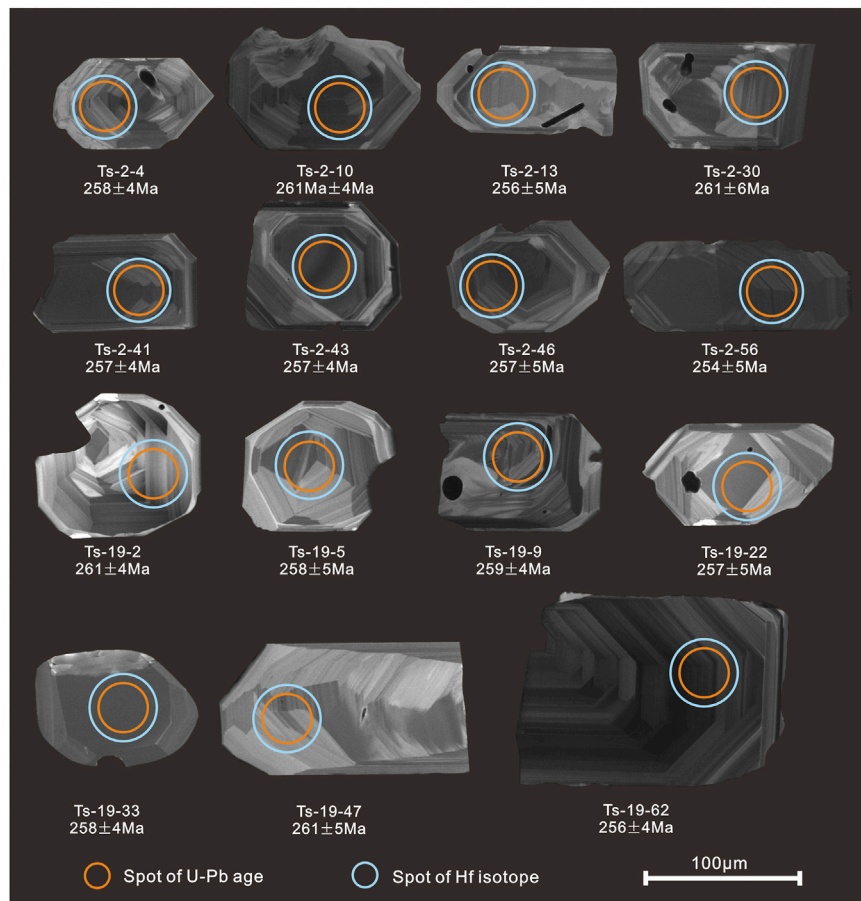


FIGURE 6 | Cathodoluminescence (CL) images of representative zircons from clastic rock samples at Dengchuan.

reduction were given in Zong et al. (2017). The analyses were performed on an Agilent 7700e ICP-MS instrument with a GeoLasPro laser ablation system that consists of a COMPexPro 102 ArF excimer laser (wavelength of 193 nm and maximum energy of 200 mJ) and a MicroLas optical system. In this study, the spot diameter and frequency of the laser were set to 32 μm and 5 Hz, respectively. Zircon 91500 was used as standards for U-Pb dating. Standard silicate glass SRM610 was used to calibrate the contents of elements. Each analysis consisted of approximately 20–30 s blank measurement and 50 s of data acquisition from the sample. Integration of background, off-line selection, analyzed signals, time-drift correction, and quantitative calibration for trace element analysis and U-Pb dating were conducted with Excel-based software ICPMSDataCal (Liu et al., 2008, 2010). All the age calculations and concordia diagrams were made using Isoplot 3.0 (Ludwig, 2003).

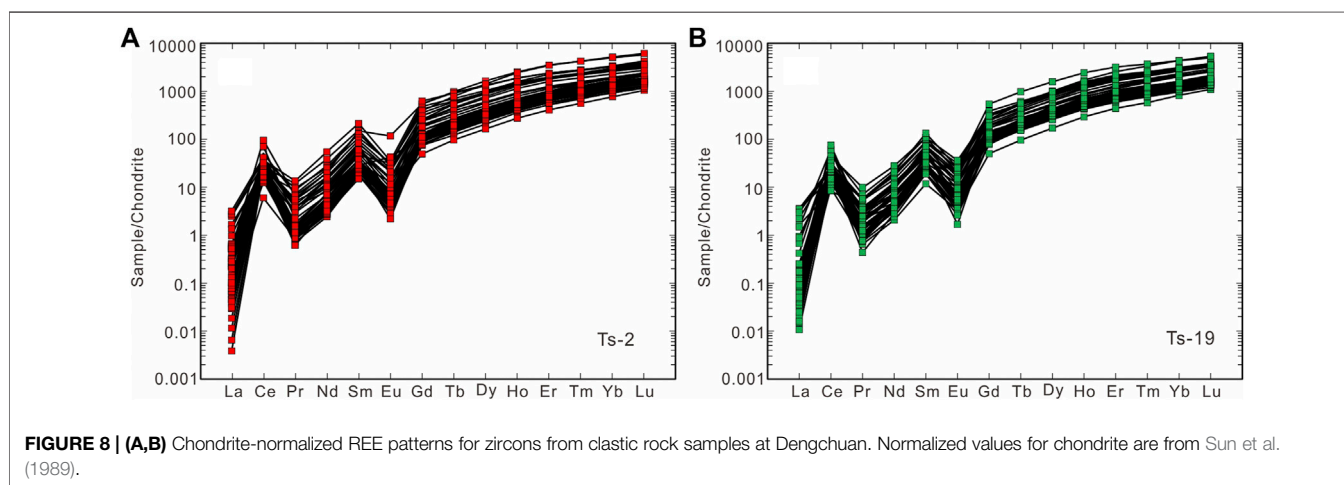
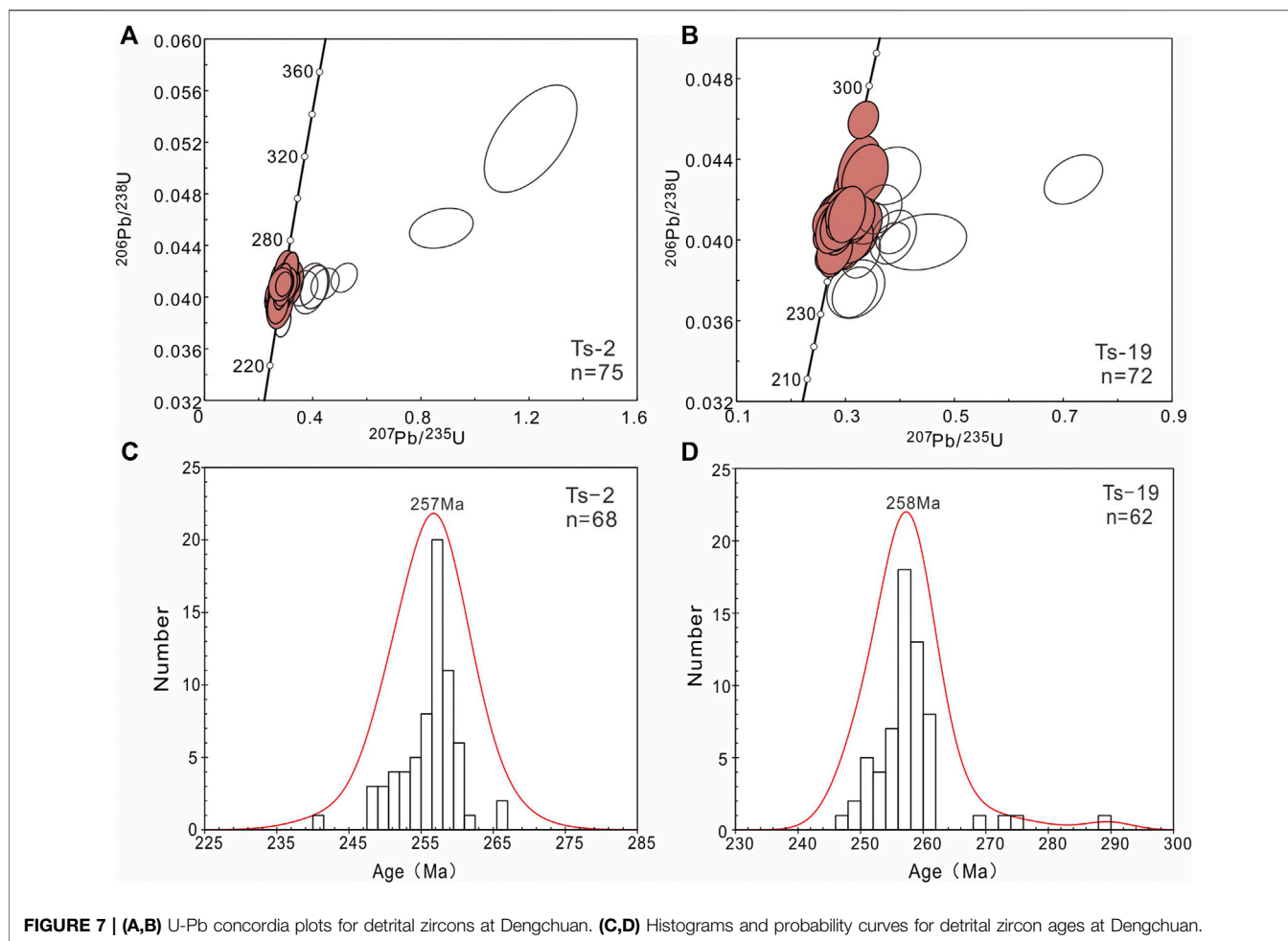
In situ zircon Hf isotopic measurements were performed using a Neptune Plus MC-ICP-MS (Thermo Fisher Scientific, Germany) in combination with a GeoLas HD excimer ArF laser ablation system (Coherent, Göttingen, Germany) at Wuhan Sample Solution Analytical Technology Co., Ltd, Wuhan, China. The Hf isotopic analyses were carried out on the same spots that were previously analyzed for U-Pb dating. The analysis parameters mainly include beam diameter of 44 μm , the ablation energy density of $\sim 7.0 \text{ J/cm}^2$,

background signal acquisition of 20 s, and ablation signal acquisition of 50 s. Detailed operating conditions and analytical methods were described by Hu et al. (2012). Zircon Plešovice, 91500, GJ-1, and TEM were analyzed as standard samples. The test value is consistent with the recommended value within the error range. Integration of analyte signals and off-line selection, and mass bias calibrations were performed using Excel-based software ICPMSDataCal (Liu et al., 2010). The decay constant of ^{176}Lu is $1.867 \times 10^{-11}/\text{year}$ (Söderlund et al., 2004). The values of $\epsilon_{\text{Hf}}(t)$ are calculated relative to chondrites whose $^{176}\text{Hf}/^{177}\text{Hf}$ and $^{176}\text{Lu}/^{177}\text{Hf}$ ratios are 0.282,772 and 0.0332, respectively (Blichert-Toft and Albarède, 1997). The single-stage model age (T_{DM1}) was calculated relative to the depleted mantle using 0.28325 for the $^{176}\text{Hf}/^{177}\text{Hf}$ ratio and 0.0384 for the $^{176}\text{Lu}/^{177}\text{Hf}$ ratio (Griffin et al., 2000). The two-stage model age (T_{DM2}) was calculated by assuming that zircon parental magma is derived from an average continental crust with a $^{176}\text{Lu}/^{177}\text{Hf}$ ratio of 0.015 (Griffin et al., 2000).

4 RESULTS

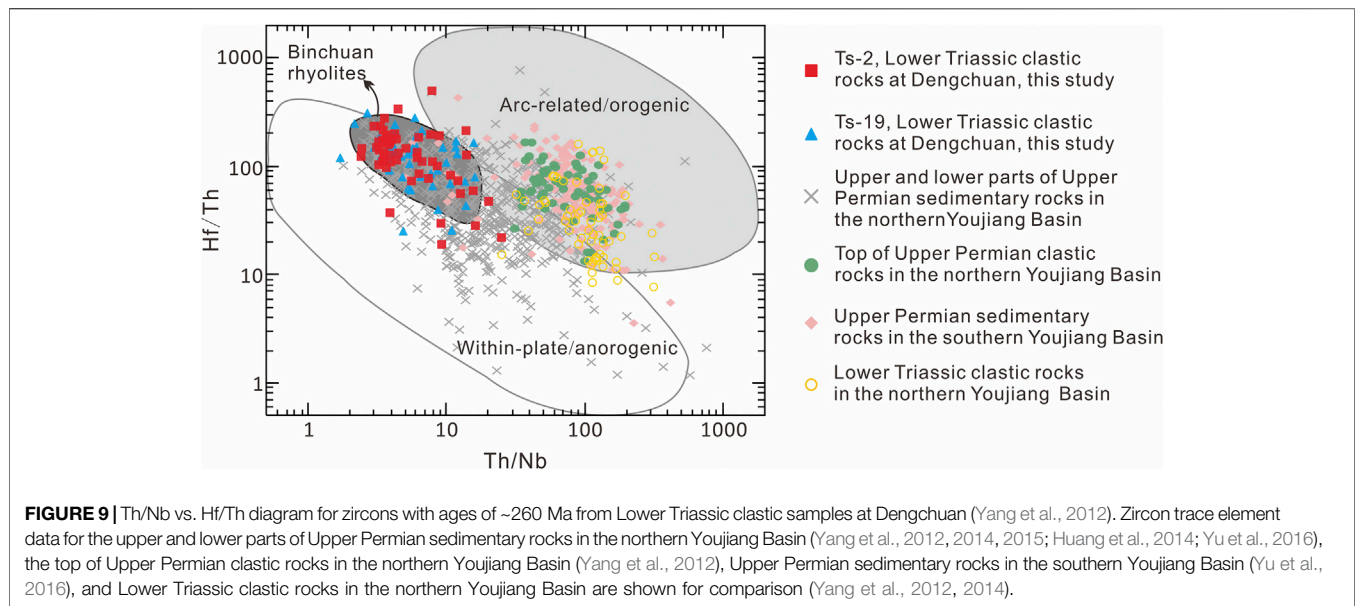
4.1 Whole-Rock Geochemistry

The mudstone samples contain variational SiO_2 (21.42–58.18%), Al_2O_3 (7.29–19.74%), TiO_2 (0.93–2.92%), and CaO (0.54–32.8%)



values, with low Na_2O values (0.01–0.64%) and high K_2O values (2.2–6.11%) (**Supplementary Table S1**). The TiO_2 values are 0.93–2.92%, which are lower than Emeishan high-Ti basalts (>2.5%) (Xiao et al., 2003, 2004; Zhou et al., 2006; Fan et al., 2008; Song et al., 2008; Xu et al., 2008; Anh et al., 2011; Lai et al.,

2012; Huang et al., 2014; He et al., 2018), but higher than Emeishan rhyolites (0.40–0.75%) (Xu et al., 2010; Cheng et al., 2017; Hei et al., 2018; Huang et al., 2022a). High CaO contents in some samples are consistent with the presence of limestone fragments in sandstone samples.



All samples have similar chondrite-normalized rare Earth element (REE) patterns with LREE enrichment and slightly negative Eu anomalies. In primitive mantle-normalized plots (Figure 5B), most of the analyzed samples show negative Sr anomaly and no Nb–Ta anomaly, similar to Emeishan high-Ti basalts and rhyolites (Figure 5B). Some samples (Ts-4, Ts-5, and Ts-9) from the upper part of the Qingtianbao Formation show slightly negative Nb–Ta anomalies, similar to the UCC (Rudnick and Gao, 2003) and arc-related magmatic rocks (Figure 5B) (Omrani et al., 2008).

4.2 Zircon U-Pb Ages

Zircon grains from sandstone samples are euhedral to subhedral and only a few grains are moderately rounded. They are 80–150 μm in length and have aspect ratios between 1:1 and 2.5:1 (Figure 6). Most zircons have oscillatory zoning without inherited core in the cathodoluminescence (CL) images and have high Th/U ratios (0.33–1.43) (Supplementary Table S2), indicating a magma origin (Hoskin and Schaltegger, 2003).

Seventy-five analyses were undertaken on 75 detrital zircon grains from the sandstone samples Ts-2, and sixty-eight ages displayed concordance greater than 90% (Figure 7A). These concordant ages range from 266 to 241 Ma, with a single peak at 257 Ma (Figure 7C).

Of 72 analyses on 72 detrital zircon grains, 62 were concordant for the sandstone sample Ts-19 (Figure 7B). The measured ages are between 290 Ma and 241 Ma, with a single peak at 258 Ma (Figure 7D).

4.3 Zircon Trace Elements

Trace elements for 103 zircon grains with ages at ~260 Ma are listed in Supplementary Table S3. Most of the analyzed grains have REE patterns that increase steeply from La to Lu, with positive Ce anomalies and negative Eu anomalies (Figure 8). Some trace element data for zircon grains were plotted on the Th/U vs. Nb/Hf diagram (Figure 9), which were constructed to distinguish the tectonic setting of the parental magma (Yang

et al., 2012). Most zircons from the Qingtianbao Formation are plotted in the within-plate/anorogenic field.

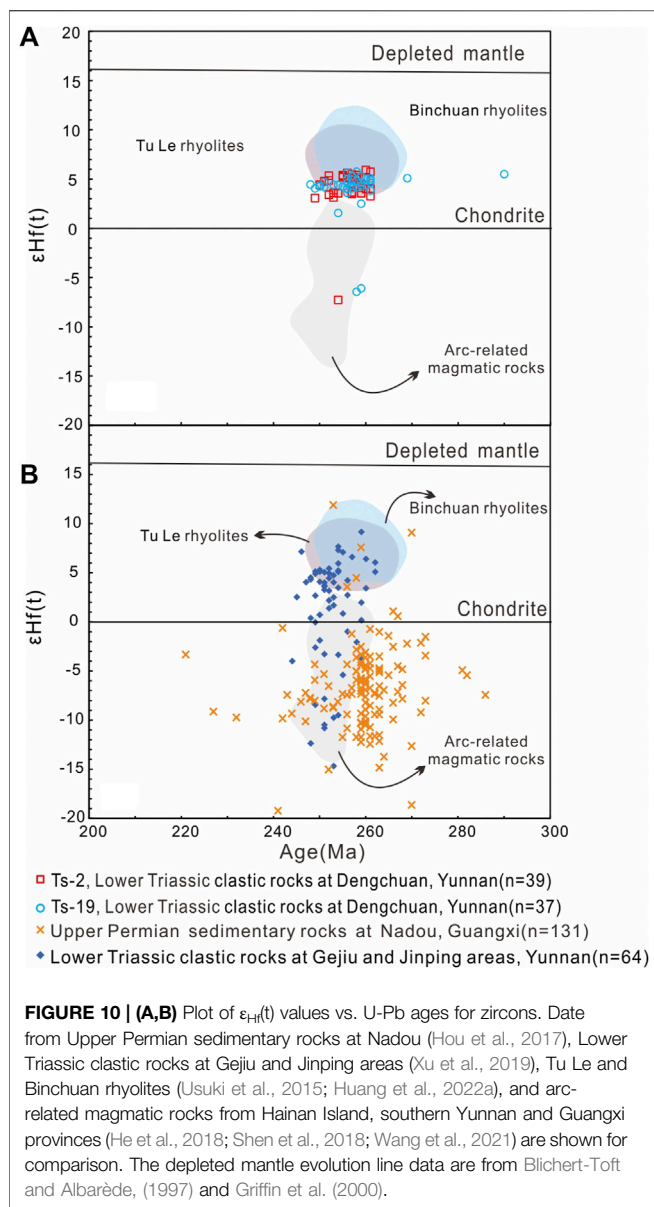
4.4 Zircons Hf Isotope

The Hf isotopic compositions for 76 zircon grains with ages ranging from 290 Ma to 248 Ma are presented in Supplementary Table S4. The results show that 73 zircon grains have positive $\epsilon_{\text{Hf}}(t)$ values ranging from +1.6 to +5.9 (Figure 10A) and two-stage model ages ranging from 1,063 to 826 Ma, while only three zircon grains have negative $\epsilon_{\text{Hf}}(t)$ values ranging from –7.3 to –6.1 (Figure 10A) and two-stage model ages ranging from 1,555 to 1,491 Ma (Supplementary Table S4).

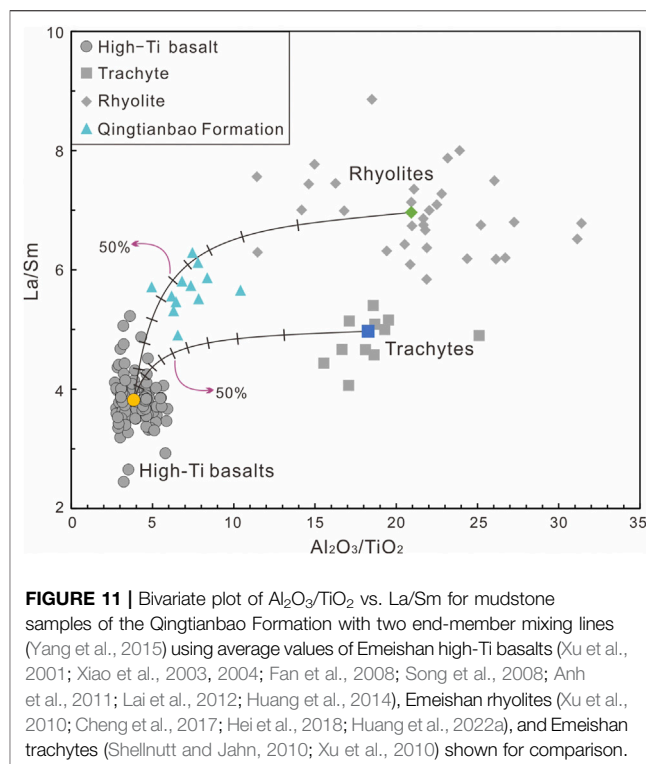
5 DISCUSSION

5.1 Provenance of Lower Triassic Succession

The studied sandstone samples from the Lower Triassic Qingtianbao Formation yielded only one predominant peak at ~260 Ma. The contemporaneous igneous activity along the southwestern margin of the South China Craton could be related to the ELIP or a convergent plate margin magmatic arc generated by the closure of the Paleotethyan or Panthalassa Ocean (Zhou et al., 2002; Li et al., 2006; Jian et al., 2009; Zhong et al., 2014). The low-Ti basalts of the ELIP are preserved at the bottom of the Emeishan volcanic succession, which were not accessible to surface erosion during the Late Permian and Early Triassic, and thus they would not be the potential source (He et al., 2007). Most studied samples are geochemically similar to Emeishan high-Ti basalts and felsic volcanic rocks (Figures 5, 7, 11) but different from the arc-related magmatic rocks (Figure 9). Some samples show similar geochemical features to the UCC and arc-related magmatic rocks (Figure 5), suggestive of a possible genetic link. However, the zircons from the studied sandstone samples mostly fall into the within-plate/anorogenic zone (Figure 9A), which is



consistent with the ELIP being derived from a mantle plume source region (Chung and Jahn, 1995; Xu et al., 2001). The positive $\epsilon_{\text{Hf}}(t)$ values in most zircons from the Lower Triassic sandstones at Dengchuan are similar to those from Emeishan rhyolites in Binchuan and Tu Le (Usuki et al., 2015; Huang et al., 2022a) but different from the arc-related magmatic rocks (most <0) reported in the Hainan Island, southern Yunnan and Guangxi provinces (He et al., 2018; Shen et al., 2018; Xu et al., 2018; Wang et al., 2021). These chemical and isotopic characteristics suggest that the sources of the Lower Triassic clastic rocks at Dengchuan are not related to arc-related magmatism but were derived from the ELIP. The nearby sources related to the ELIP are consistent with the euhedral/prismatic crystal morphology for most analyzed zircons. The presence of basaltic and felsic volcanic lithic fragments in sandstone samples indicates that the sources of clastic rocks in the Qingtianbao Formation are a mixture of mafic and felsic rocks. This is consistent with the unconformity



contact of the Lower Triassic clastic rocks with Emeishan rhyolites and high-Ti basalts at the Binchuan and Dengchuan areas. (Huang et al., 2022a; this study). Using average compositions of Emeishan high-Ti basalts (Xu et al., 2001; Xiao et al., 2003, 2004; Fan et al., 2008; Song et al., 2008; Anh et al., 2011; Lai et al., 2012; Huang et al., 2014), rhyolites (Xu et al., 2010; Cheng et al., 2017; Hei et al., 2018; Huang et al., 2022a), and trachytes (Shellnutt and Jahn, 2010; Xu et al., 2010), two end-member mixing calculations based on weathering-insensitive but source-responsive $\text{Al}_2\text{O}_3/\text{TiO}_2$ and La/Sm ratios (Yang et al., 2014, 2015) indicate that rhyolites and high-Ti basalts may be the most possible sources with similar weight percentages for detritus in the analyzed samples (Figure 11).

5.2 Indication of Subduction Polarity by Provenance

The southwestern margin of the South China Craton and Indochina Block have developed abundant magmatic rocks with ages of ~ 300 – 200 Ma (Figure 1), which are related to opening and closure of the Paleo-Tethyan or Panthalassa Ocean and ELIP (Zhou et al., 2002; Li et al., 2006; Jian et al., 2009; Zi et al., 2012; Zhong et al., 2014; Hu et al., 2017; Huang et al., 2022b). The subduction of the Panthalassa Ocean plate has been demonstrated beneath the eastern–southeastern margin of the South China Craton during the Paleozoic to Mesozoic (Isozaki et al., 2010; Hu et al., 2015a). The Permian arc-related magmatic units in Hainan Island are inferred to represent the southwest extension of this Paleozoic to Mesozoic accretionary belt (Li et al., 2006; Hu et al., 2015b). The arc-related magmatic

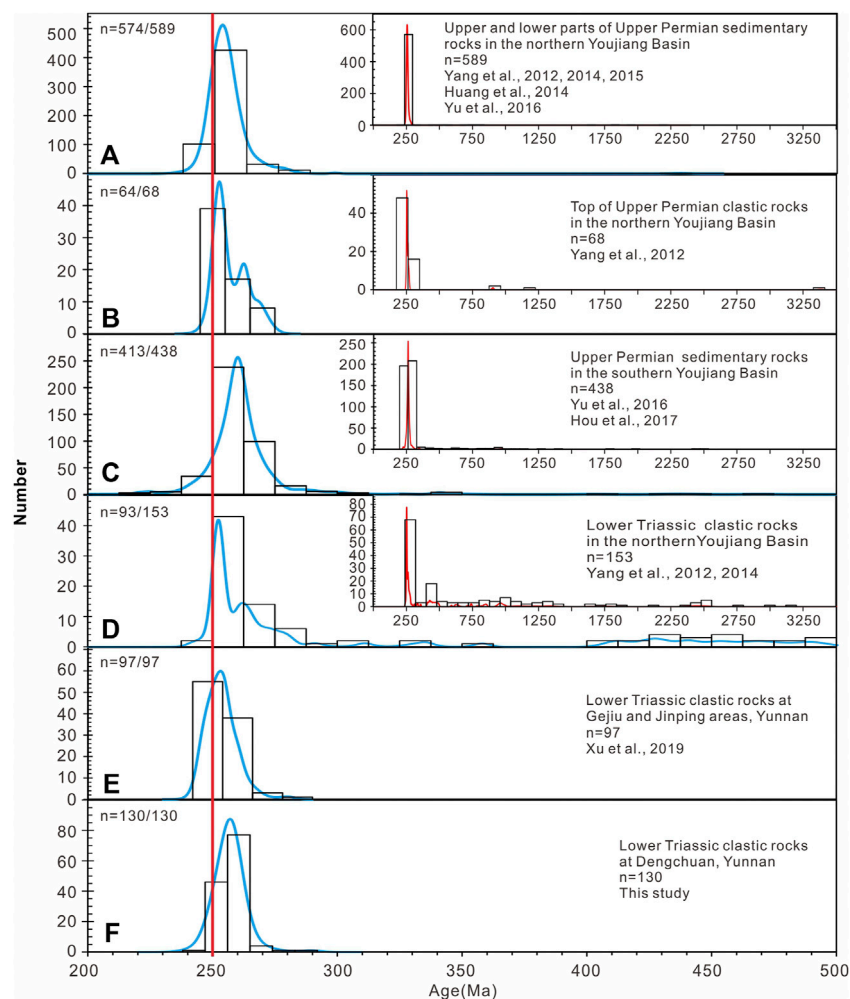
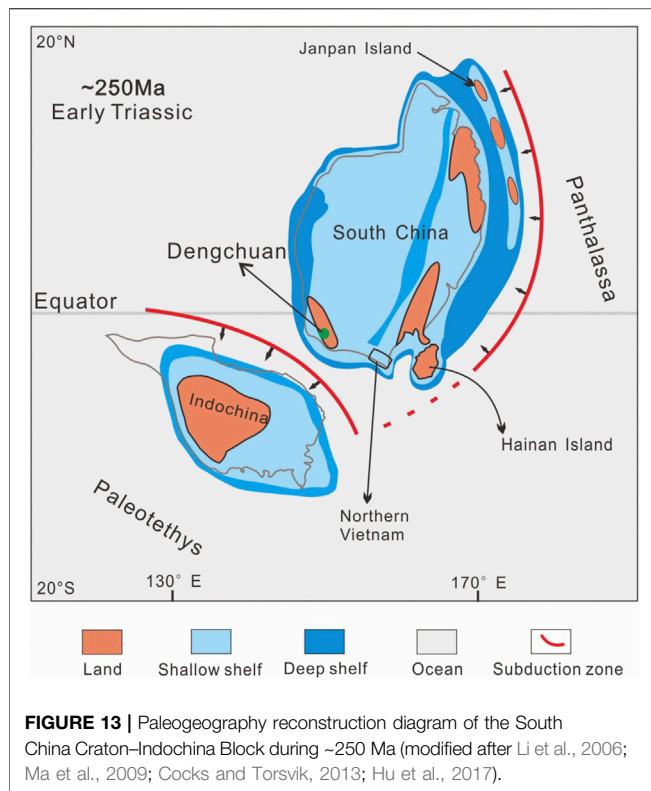


FIGURE 12 | (A–F) Probability density diagram comparing detrital zircon age patterns in the Upper Permian–Lower Triassic succession from the southwestern margin of the South China Craton.

rocks with ages of ~298–246 Ma (Jian et al., 2009; Liu et al., 2011; Li et al., 2012; Lai et al., 2014; Liu et al., 2017; He et al., 2020) were reported in the eastern Indochina Block, indicating the westward subduction of the Paleo-Tethyan Ocean. However, it is still debated whether the Paleo-Tethyan Ocean has undergone a subduction eastward beneath the South China Craton.

Detrital zircons with the main peak at ~260–250 Ma were widely reported in the Late Permian to Early Triassic strata from the southwestern margin of the South China Craton (Figures 1, 12) (Yang et al., 2012, 2014, 2015; Huang et al., 2014; Yu et al., 2016; Hou et al., 2017; Xu et al., 2019). Zircons from the upper and lower parts of Upper Permian sedimentary rocks in the northern Youjiang Basin are mostly plotted in the within-plate/anorogenic field (Figure 9) and were derived from the Emeishan volcanic rocks (Yang et al., 2012, 2014, 2015; Huang et al., 2014; Yu et al., 2016). However, zircons from the top of Upper Permian and Lower Triassic clastic rocks in the northern Youjiang Basin (Yang et al., 2012, 2014) and Upper Permian sedimentary rocks in the southern Youjiang Basin (Yu et al., 2016) are mostly plotted in

the arc-related/orogenic field (Figure 9). Most of these zircons have negative $\epsilon_{\text{Hf}}(t)$ values (Figure 10) (Hou et al., 2017), similar to those from arc-related magmatic rocks (most <0) in the Hainan Island, southern Yunnan and Guangxi provinces (Figure 1) (He et al., 2018; Shen et al., 2018; Xu et al., 2018; Wang et al., 2021). This indicates that the detritus was likely to have been derived from arc-related magmatic rock. Both abundant negative and positive $\epsilon_{\text{Hf}}(t)$ values for detrital zircons with ages of ~260 Ma are present in Lower Triassic clastic rocks at the Gejiu and Jinping areas, southern Yunnan province (Xu et al., 2019), indicating that the detritus was likely derived from a mixture of arc-related and ELIP-related magmatic rocks. The arc-related magmatic rocks have been inferred to generate from the subduction of the Paleo-Tethyan Ocean (Hou et al., 2017; Xu et al., 2019). However, recent studies about arc-related mafic rocks with ages of 254–250 Ma from the Gulinjing–Nanxi area in southern Yunnan province suggested that the subduction was linked to the Panthalassa Ocean to the south and not the Paleo-Tethyan Ocean to the west (Figure 1)



(Wang et al., 2021). The Lower Triassic clastic rocks at Dengchuan were sourced from the Emeishan volcanic rocks and not from the arc-related magmatic rocks. This is consistent with no Permian–Triassic arc-related magmatic rocks found in the western margin of the South China Craton (Wang et al., 2021). Our results do not support the eastward subduction of the Paleo-Tethyan Ocean, and the southwestern margin of the South China Craton may be a passive continental margin during the Late Permian–Early Triassic (Figure 13).

6 CONCLUSION

Provenance studies indicate that the Lower Triassic clastic rocks at Dengchuan were mainly derived from Emeishan volcanic

REFERENCES

- Ali, J. R., Fitton, J. G., and Herzberg, C. (2010). Emeishan Large Igneous Province (SW China) and the Mantle-Plume Up-Doming Hypothesis. *J. Geol. Soc.* 167 (5), 953–959. doi:10.1144/0016-76492009-129
- Anh, T. V., Pang, K.-N., Chung, S.-L., Lin, H.-M., Hoa, T. T., Anh, T. T., et al. (2011). The Song Da Magmatic Suite Revisited: A Petrologic, Geochemical and Sr-Nd Isotopic Study on Picrites, Flood Basalts and Silicic Volcanic Rocks. *J. Asian Earth Sci.* 42 (6), 1341–1355. doi:10.1016/j.jseas.2011.07.020
- Blichert-Toft, J., and Albarède, F. (1997). The Lu-Hf Isotope Geochemistry of Chondrites and the Evolution of the Mantle-Crust System. *Earth Planet. Sci. Lett.* 148 (1), 243–258. doi:10.1016/S0012-821X(97)00040-X

rocks, with a mixture of high-Ti basalts and rhyolites. Integration of our data with those from Late Permian–Early Triassic strata and magmatic rocks along the southwestern margin of the South China Craton suggests that the Paleo-Tethyan Ocean may undergo a unidirectional subduction westward beneath the Indochina Block during the Late Permian–Early Triassic.

DATA AVAILABILITY STATEMENT

The original contributions presented in the study are included in the article/**Supplementary Material**; further inquiries can be directed to the corresponding author.

AUTHOR CONTRIBUTIONS

CH: writing—original draft, investigation, and data curation. HH: conceptualization, writing—review and editing, supervision, investigation, and funding acquisition. CY: writing—review and editing and investigation. LW: writing—review and editing and investigation. HL: writing—review and editing.

FUNDING

This work was supported by the National Natural Science Foundation of China (41972103).

ACKNOWLEDGMENTS

We would like to thank Associate Editor Shengyao Yu and two anonymous reviewers for their constructive comments and suggestions, which substantially improved our manuscript.

SUPPLEMENTARY MATERIAL

The Supplementary Material for this article can be found online at: <https://www.frontiersin.org/articles/10.3389/feart.2022.932486/full#supplementary-material>

- Cawood, P. A., Hawkesworth, C. J., and Dhuime, B. (2012). Detrital Zircon Record and Tectonic Setting. *Geology* 40 (10), 875–878. doi:10.1130/G32945.1
- Cawood, P. A., Zhao, G., Yao, J., Wang, W., Xu, Y., and Wang, Y. (2018). Reconstructing South China in Phanerozoic and Precambrian Supercontinents. *Earth-Science Rev.* 186, 173–194. doi:10.1016/j.earscirev.2017.06.001
- Chen, Z., Lin, W., Faure, M., Lepvrier, C., Van Vuong, N., and Van Tich, V. (2014). Geochronology and Isotope Analysis of the Late Paleozoic to Mesozoic Granitoids from Northeastern Vietnam and Implications for the Evolution of the South China Block. *J. Asian Earth Sci.* 86, 131–150. doi:10.1016/j.jseas.2013.07.039
- Cheng, L.-L., Wang, Y., Herrin, J. S., Ren, Z.-Y., and Yang, Z.-F. (2017). Origin of K-Feldspar Megacrysts in Rhyolites from the Emeishan Large Igneous Province, Southwest China. *Lithos* 294–295, 397–411. doi:10.1016/j.lithos.2017.10.018

- Chung, S.-L., and Jahn, B.-M. (1995). Plume-lithosphere Interaction in Generation of the Emeishan Flood Basalts at the Permian-Triassic Boundary. *Geol* 23 (10), 889–892. doi:10.1130/0091-7613(1995)023<0889:PLIIGO>2.3.CO
- Cocks, L. R. M., and Torsvik, T. H. (2013). The Dynamic Evolution of the Palaeozoic Geography of Eastern Asia. *Earth-Science Rev.* 117, 40–79. doi:10.1016/j.earscirev.2012.12.001
- Fan, W., Wang, Y., Zhang, A., Zhang, F., and Zhang, Y. (2010). Permian Arc-Back-Arc Basin Development along the Ailaoshan Tectonic Zone: Geochemical, Isotopic and Geochronological Evidence from the Mojiang Volcanic Rocks, Southwest China. *Lithos* 119 (3–4), 553–568. doi:10.1016/j.lithos.2010.08.010
- Fan, W., Zhang, C., Wang, Y., Guo, F., and Peng, T. (2008). Geochronology and Geochemistry of Permian Basalts in Western Guangxi Province, Southwest China: Evidence for Plume-Lithosphere Interaction. *Lithos* 102 (1–2), 218–236. doi:10.1016/j.lithos.2007.09.019
- Faure, M., Lepvrier, C., Nguyen, V. V., Vu, T. V., Lin, W., and Chen, Z. (2014). The South China Block-Indochina Collision: where, when, and How? *J. Asian Earth Sci.* 79, 260–274. doi:10.1016/j.jseas.2013.09.022
- Gan, C., Wang, Y., Zhang, Y., Qian, X., and Zhang, A. (2021). The Assembly of the South China and Indochina Blocks: Constraints from the Triassic Felsic Volcanics in the Youjiang Basin. *Geol. Soc. Am. Bull.* 133 (9–10), 2097–2112. doi:10.1130/B35816.1
- Griffin, W. L., Pearson, N. J., Belousova, E., Jackson, S. E., van Achterbergh, E., O'Reilly, S. Y., et al. (2000). The Hf Isotope Composition of Cratonic Mantle: LAM-MC-ICPMS Analysis of Zircon Megacrysts in Kimberlites. *Geochimica Cosmochimica Acta* 64 (1), 133–147. doi:10.1016/S0016-7037(99)00343-9
- Halpin, J. A., Tran, H. T., Lai, C.-K., Meffre, S., Crawford, A. J., and Zaw, K. (2016). U-pb Zircon Geochronology and Geochemistry from NE Vietnam: A 'tectonically Disputed' Territory between the Indochina and South China Blocks. *Gondwana Res.* 34, 254–273. doi:10.1016/j.gr.2015.04.005
- He, B., Xu, Y.-G., Huang, X.-L., Luo, Z.-Y., Shi, Y.-R., Yang, Q.-J., et al. (2007). Age and Duration of the Emeishan Flood Volcanism, SW China: Geochemistry and SHRIMP Zircon U-Pb Dating of Silicic Ignimbrites, Post-volcanic Xuanwei Formation and Clay Tuff at the Chaotian Section. *Earth Planet. Sci. Lett.* 255 (3–4), 306–323. doi:10.1016/j.epsl.2006.12.021
- He, H., Wang, Y., Cawood, P. A., Qian, X., Zhang, Y., and Zhao, G. (2020). Permo-Triassic Granitoids, Hainan Island, Link to Paleotethyan Not Paleopacific Tectonics. *Geol. Soc. Am. Bull.* 132 (9–10), 2067–2083. doi:10.1130/B35370.1
- He, H., Wang, Y., Qian, X., and Zhang, Y. (2018). The Bangxi-Chenxing Tectonic Zone in Hainan Island (South China) as the Eastern Extension of the Song Ma-Ailaoshan Zone: Evidence of Late Paleozoic and Triassic Igneous Rocks. *J. Asian Earth Sci.* 164, 274–291. doi:10.1016/j.jseas.2018.06.032
- Hei, H.-X., Su, S.-G., Wang, Y., Mo, X.-X., Luo, Z.-H., and Liu, W.-G. (2018). Rhyolites in the Emeishan Large Igneous Province (SW China) with Implications for Plume-Related Felsic Magmatism. *J. Asian Earth Sci.* 164, 344–365. doi:10.1016/j.jseas.2018.05.032
- Hoa, T. T., Izokh, A. E., Polyakov, G. V., Borisenko, A. S., Anh, T. T., Balykin, P. A., et al. (2008). Permo-Triassic Magmatism and Metallogeny of Northern Vietnam in Relation to the Emeishan Plume. *Russ. Geol. Geophys.* 49 (7), 480–491. doi:10.1016/j.rgg.2008.06.005
- Hoskin, P. W. O., and Schaltegger, U. (2003). 2. The Composition of Zircon and Igneous and Metamorphic Petrogenesis. *Rev. Mineral. Geochem.* 53 (1), 27–62. doi:10.1515/9781501509322-005
- Hou, Y.-l., Zhong, Y.-t., Xu, Y.-g., and He, B. (2017). The Provenance of Late Permian Karstic Bauxite Deposits in SW China, Constrained by the Geochemistry of Interbedded Clastic Rocks, and U-Pb-Hf-O Isotopes of Detrital Zircons. *Lithos* 278–281, 240–254. doi:10.1016/j.lithos.2017.01.013
- Hou, Z.-s., Fan, J.-x., Henderson, C. M., Yuan, D.-x., Shen, B.-h., Wu, J., et al. (2020). Dynamic Palaeogeographic Reconstructions of the Wuchiapingian Stage (Lopingian, Late Permian) for the South China Block. *Palaeogeogr. Palaeoclimatol. Palaeoecol.* 546, 109667. doi:10.1016/j.palaeo.2020.109667
- Hu, L., Cawood, P. A., Du, Y., Xu, Y., Wang, C., Wang, Z., et al. (2017). Permo-Triassic Detrital Records of South China and Implications for the Indosinian Events in East Asia. *Palaeogeogr. Palaeoclimatol. Palaeoecol.* 485, 84–100. doi:10.1016/j.palaeo.2017.06.005
- Hu, L., Cawood, P. A., Du, Y., Xu, Y., Xu, W., and Huang, H. (2015b). Detrital Records for Upper Permian-Lower Triassic Succession in the Shiwandashan Basin, South China and Implication for Permo-Triassic (Indosinian) Orogeny. *J. Asian Earth Sci.* 98, 152–166. doi:10.1016/j.jseas.2014.11.007
- Hu, L., Cawood, P. A., Du, Y., Yang, J., and Jiao, L. (2015a). Late Paleozoic to Early Mesozoic Provenance Record of Paleo-Pacific Subduction beneath South China. *Tectonics* 34 (5), 986–1008. doi:10.1002/2014TC003803
- Hu, Z., Liu, Y., Gao, S., Liu, W., Zhang, W., Tong, X., et al. (2012). Improved *In Situ* Hf Isotope Ratio Analysis of Zircon Using Newly Designed X Skimmer Cone and Jet Sample Cone in Combination with the Addition of Nitrogen by Laser Ablation Multiple Collector ICP-MS. *J. Anal. At. Spectrom.* 27 (9), 1391–1399. doi:10.1039/c2ja30078h
- Huang, H., Cawood, P. A., Hou, M.-C., Ni, S.-J., Yang, J.-H., Du, Y.-S., et al. (2018). Provenance of Late Permian Volcanic Ash Beds in South China: Implications for the Age of Emeishan Volcanism and its Linkage to Climate Cooling. *Lithos* 314–315, 293–306. doi:10.1016/j.lithos.2018.06.009
- Huang, H., Cawood, P. A., Hou, M.-C., Xiong, F.-H., Ni, S.-J., Deng, M., et al. (2022a). Zircon U-Pb Age, Trace Element, and Hf Isotopic Constrains on the Origin and Evolution of the Emeishan Large Igneous Province. *Gondwana Res.* 105, 535–550. doi:10.1016/j.gr.2021.09.023
- Huang, H., Cawood, P. A., Hou, M.-C., Yang, J.-H., Ni, S.-J., Du, Y.-S., et al. (2016). Silicic Ash Beds Bracket Emeishan Large Igneous Province to < 1 m.Y. At ~ 260 Ma. *Lithos* 264, 17–27. doi:10.1016/j.lithos.2016.08.013
- Huang, H., Du, Y.-S., Yang, J.-H., Zhou, L., Hu, L.-S., Huang, H.-W., et al. (2014). Origin of Permian Basalts and Clastic Rocks in Napo, Southwest China: Implications for the Erosion and Eruption of the Emeishan Large Igneous Province. *Lithos* 208–209, 324–338. doi:10.1016/j.lithos.2014.09.022
- Huang, H., Huyskens, M., Yin, Q. Z., Cawood, P. A., Hou, M. C., Yang, J. H., et al. (2022b). *Eruptive Tempo of Emeishan Large Igneous Province, Southwestern China and Northern Vietnam: Relations to Biotic Crises and Paleoclimate Changes Around the Guadalupian-Lopingian Boundary.* *Geology.* In Press. doi:10.1130/G50183.1
- Isozaki, Y., Aoki, K., Nakama, T., and Yanai, S. (2010). New Insight into a Subduction-Related Orogen: A Reappraisal of the Geotectonic Framework and Evolution of the Japanese Islands. *Gondwana Res.* 18 (1), 82–105. doi:10.1016/j.gr.2010.02.015
- Jian, P., Liu, D., Kröner, A., Zhang, Q., Wang, Y., Sun, X., et al. (2009). Devonian to Permian Plate Tectonic Cycle of the Paleo-Tethys Orogen in Southwest China (II): Insights from Zircon Ages of Ophiolites, Arc/back-Arc Assemblages and Within-Plate Igneous Rocks and Generation of the Emeishan CFB Province. *Lithos* 113 (3–4), 767–784. doi:10.1016/j.lithos.2009.04.006
- Lai, C.-K., Meffre, S., Crawford, A. J., Zaw, K., Xue, C.-D., and Halpin, J. A. (2014). The Western Ailaoshan Volcanic Belts and Their SE Asia Connection: A New Tectonic Model for the Eastern Indochina Block. *Gondwana Res.* 26 (1), 52–74. doi:10.1016/j.gr.2013.03.003
- Lai, S., Qin, J., Li, Y., Li, S., and Santosh, M. (2012). Permian High Ti/Y Basalts from the Eastern Part of the Emeishan Large Igneous Province, Southwestern China: Petrogenesis and Tectonic Implications. *J. Asian Earth Sci.* 47, 216–230. doi:10.1016/j.jseas.2011.07.010
- Li, G., Li, C., Ripley, E. M., Kamo, S., and Su, S. (2012). Geochronology, Petrology and Geochemistry of the Nanlinshan and Banpo Mafic-Ultramafic Intrusions: Implications for Subduction Initiation in the Eastern Paleo-Tethys. *Contrib. Mineral. Pet.* 164 (5), 773–788. doi:10.1007/s00410-012-0770-4
- Li, Q., Lin, W., Wang, Y., Faure, M., Meng, L., Wang, H., et al. (2021). Detrital Zircon U Pb Age Distributions and Hf Isotopic Constraints of the Ailaoshan-Song Ma Suture Zone and Their Paleogeographic Implications for the Eastern Paleo-Tethys Evolution. *Earth-Science Rev.* 221, 103789. doi:10.1016/j.earscirev.2021.103789
- Li, X.-H., Li, W.-X., Li, Z.-X., Lo, C.-H., Wang, J., Ye, M.-F., et al. (2009). Amalgamation between the Yangtze and Cathaysia Blocks in South China: Constraints from SHRIMP U-Pb Zircon Ages, Geochemistry and Nd-Hf Isotopes of the Shuangxiwu Volcanic Rocks. *Precambrian Res.* 174 (1–2), 117–128. doi:10.1016/j.precambres.2009.07.004
- Li, X. H., Li, Z. X., Li, W. X., and Wang, Y. (2006). Initiation of the Indosinian Orogeny in South China: Evidence for a Permian Magmatic Arc on Hainan Island. *J. Geol.* 114 (3), 341–353. doi:10.1086/501222
- Liu, B. J., and Xu, X. S. (1994). *Atlas of Lithofacies and Palaeogeography of South China (Simian to Triassic).* Beijing: Science Press. (in Chinese).
- Liu, B., Ma, C.-Q., Guo, P., Sun, Y., Gao, K., and Guo, Y.-H. (2016). Evaluation of Late Permian Mafic Magmatism in the Central Tibetan Plateau as a Response to Plume-Subduction Interaction. *Lithos* 264, 1–16. doi:10.1016/j.lithos.2016.08.011

- Liu, C., Deng, J. F., Liu, J. L., and Shi, Y. L. (2011). Characteristics of Volcanic Rocks from Late Permian to Early Triassic in Ailaoshan Tectono-magmatic Belt and Implications for Tectonic Settings. *Acta Pet. Sin.* 12 (27), 3590. (In Chinese With English Abstract).
- Liu, H., Wang, Y., and Zi, J.-W. (2017). Petrogenesis of the Dalongkai Ultramafic-Mafic Intrusion and its Tectonic Implication for the Paleotethyan Evolution along the Ailaoshan Tectonic Zone (SW China). *J. Asian Earth Sci.* 141, 112–124. doi:10.1016/j.jseas.2016.07.015
- Liu, Y., Gao, S., Hu, Z., Gao, C., Zong, K., and Wang, D. (2010). Continental and Oceanic Crust Recycling-Induced Melt-Peridotite Interactions in the Trans-North China Orogen: U-Pb Dating, Hf Isotopes and Trace Elements in Zircons from Mantle Xenoliths. *J. Petrology* 51 (1-2), 537–571. doi:10.1093/petrology/egp082
- Liu, Y., Hu, Z., Gao, S., Günther, D., Xu, J., Gao, C., et al. (2008). *In Situ* analysis of Major and Trace Elements of Anhydrous Minerals by LA-ICP-MS without Applying an Internal Standard. *Chem. Geol.* 257 (1-2), 34–43. doi:10.1016/j.chemgeo.2008.08.004
- Ludwig, K. R. (2003). *User's Manual for Isoplot 3.00: A Geochronological Toolkit for Microsoft Excel*. California Berkeley: Berkeley Geochronology Center, p39.
- Ma, Q., Zheng, J., Griffin, W. L., Zhang, M., Tang, H., Su, Y., et al. (2012). Triassic "Adakitic" Rocks in an Extensional Setting (North China): Melts from the Cratonic Lower Crust. *Lithos* 149, 159–173. doi:10.1016/j.lithos.2012.04.017
- Ma, Y. S., Chen, H. D., and Wang, G. L. (2009). *Tectonic-sequence Lithofacies Palaeogeography Atlas of South China: Sinian-Neogene*. Beijing: Science Press. (In Chinese).
- Metcalfe, I. (2013). Gondwana Dispersion and Asian Accretion: Tectonic and Palaeogeographic Evolution of Eastern Tethys. *J. Asian Earth Sci.* 66, 1–33. doi:10.1016/j.jseas.2012.12.020
- Metcalfe, I. (2006). Palaeozoic and Mesozoic Tectonic Evolution and Palaeogeography of East Asian Crustal Fragments: The Korean Peninsula in Context. *Gondwana Res.* 9 (1-2), 24–46. doi:10.1016/j.gr.2005.04.002
- Ngo, T. X., Santosh, M., Tran, H. T., and Pham, H. T. (2016). Subduction Initiation of Indochina and South China Blocks: Insight from the Forearc Ophiolitic Peridotites of the Song Ma Suture Zone in Vietnam. *Geol. J.* 51 (3), 421–442. doi:10.1002/gj.2640
- Omrani, J., Agard, P., Whitechurch, H., Benoit, M., Prouteau, G., and Jolivet, L. (2008). Arc-magmatism and Subduction History beneath the Zagros Mountains, Iran: A New Report of Adakites and Geodynamic Consequences. *Lithos* 106 (3-4), 380–398. doi:10.1016/j.lithos.2008.09.008
- Qing, X. F., Wang, Z. Q., Zhang, Y. L., Pan, L. Z., Hu, G. A., and Zhou, F. S. (2011). Geochronology and Geochemistry of Early Mesozoic Acidic Volcanic Rocks in Sw Guangxi: Constraints on Tectonic Evolution of the Sw Qin-Hang Boundary Zone. *Acta Pet. Sin.* 27 (03), 794 (In Chinese With English Abstract).
- Rudnick, R. L., and Gao, S. (2003). Composition of the Continental Crust. *Treat. Geochem.* 3, 1–64. doi:10.1016/B0-08-043751-6/03016-4
- Scholl, D. W., and von Huene, R. (2009). Implications of Estimated Magmatic Additions and Recycling Losses at the Subduction Zones of Accretionary (Non-collisional) and Collisional (Suturing) Orogens. *Geol. Soc. Lond. Spec. Publ.* 318 (1), 105–125. doi:10.1144/SP318.4
- Shellnutt, J. G., Denyszyn, S. W., and Mundil, R. (2012). Precise Age Determination of Mafic and Felsic Intrusive Rocks from the Permian Emeishan Large Igneous Province (SW China). *Gondwana Res.* 22 (1), 118–126. doi:10.1016/j.gr.2011.10.009
- Shellnutt, J. G., and Jahn, B.-M. (2010). Formation of the Late Permian Panzhihua Plutonic-Hypabyssal-Volcanic Igneous Complex: Implications for the Genesis of Fe-Ti Oxide Deposits and A-type Granites of SW China. *Earth Planet. Sci. Lett.* 289 (3-4), 509–519. doi:10.1016/j.epsl.2009.11.044
- Shellnutt, J. G., Pham, T. T., Denyszyn, S. W., Yeh, M.-W., and Tran, T.-A. (2020). Magmatic Duration of the Emeishan Large Igneous Province: Insight from Northern Vietnam. *Geology* 48 (5), 457–461. doi:10.1130/G47076.1
- Shen, L., Yu, J.-H., O'Reilly, S. Y., Griffin, W. L., and Zhou, X. (2018). Subduction-related Middle Permian to Early Triassic Magmatism in Central Hainan Island, South China. *Lithos* 318-319, 158–175. doi:10.1016/j.lithos.2018.08.009
- Söderlund, U., Patchett, P. J., Vervoort, J. D., and Isachsen, C. E. (2004). The ¹⁷⁶Lu Decay Constant Determined by Lu-Hf and U-Pb Isotope Systematics of Precambrian Mafic Intrusions. *Earth Planet. Sc. Lett.* 219 (3-4), 311–324. doi:10.1016/S0012-821X(04)00012-3
- Song, X.-Y., Qi, H.-W., Robinson, P. T., Zhou, M.-F., Cao, Z.-M., and Chen, L.-M. (2008). Melting of the Subcontinental Lithospheric Mantle by the Emeishan Mantle Plume; Evidence from the Basal Alkaline Basalts in Dongchuan, Yunnan, Southwestern China. *Lithos* 100 (1-4), 93–111. doi:10.1016/j.lithos.2007.06.023
- Sun, S.-s., McDonough, W. F., Saunders, A. D., and Norry, M. J. (1989). Chemical and Isotopic Systematics of Oceanic Basalts: Implications for Mantle Composition and Processes. *Geol. Soc. Lond. Spec. Publ.* 42 (1), 313–345. doi:10.1144/GSL.SP.1989.042.01.19
- Tran, T. V., Faure, M., Nguyen, V. V., Bui, H. H., Fyhn, M. B. W., Nguyen, T. Q., et al. (2020). Neoproterozoic to Early Triassic Tectono-Stratigraphic Evolution of Indochina and Adjacent Areas: A Review with New Data. *J. Asian Earth Sci.* 191, 104231. doi:10.1016/j.jseas.2020.104231
- Usuki, T., Lan, C.-Y., Tran, T. H., Pham, T. D., Wang, K.-L., Shellnutt, G. J., et al. (2015). Zircon U-Pb Ages and Hf Isotopic Compositions of Alkaline Silicic Magmatic Rocks in the Phan Si Pan-Tu Le Region, Northern Vietnam: Identification of a Displaced Western Extension of the Emeishan Large Igneous Province. *J. Asian Earth Sci.* 97, 102–124. doi:10.1016/j.jseas.2014.10.016Wang
- Wang, Y., Wang, Q., Deng, J., Xue, S., Li, C., and Ripley, E. M. (2021). Late Permian-Early Triassic Mafic Dikes in the Southwestern Margin of the South China Block: Evidence for Paleo-Pacific Subduction. *Lithos* 384-385, 105994. doi:10.1016/j.lithos.2021.105994
- Xia, X.-P., Xu, J., Huang, C., Long, X., and Zhou, M. (2019). Subduction Polarity of the Ailaoshan Ocean (Eastern Paleotethys): Constraints from Detrital Zircon U-Pb and Hf-O Isotopes for the Longtan Formation. *Geol. Soc. Am. Bull.* 132 (5-6), 987–996. doi:10.1130/B35294.1
- Xiao, L., Xu, Y.-G., Chung, S.-L., He, B., and Mei, H. (2003). Chemostratigraphic Correlation of Upper Permian Lavas from Yunnan Province, China: Extent of the Emeishan Large Igneous Province. *Int. Geol. Rev.* 45 (8), 753–766. doi:10.2747/0020-6814.45.8.753
- Xiao, L., Xu, Y. G., Mei, H. J., Zheng, Y. F., He, B., and Pirajno, F. (2004). Distinct Mantle Source of Low-Ti and High-Ti Basalts from the Western Emeishan Large Igneous Province, SW China: Implications for Plume-Lithosphere Interaction. *Earth Planet. Sci. Lett.* 228 (3-4), 525–546. doi:10.1016/j.epsl.2004.10.002
- Xu, J., Xia, X. P., Lai, C., Long, X., and Huang, C. (2019). When Did the Paleotethys Ailaoshan Ocean Close: New Insights from Detrital Zircon U-Pb Age and Hf Isotopes. *Tectonics* 38 (5), 1798–1823. doi:10.1029/2018TC005291
- Xu, W.-C., Luo, B.-J., Xu, Y.-J., Wang, L., and Chen, Q. (2018). Geochronology, Geochemistry, and Petrogenesis of Late Permian to Early Triassic Mafic Rocks from Darongshan, South China: Implications for Ultrahigh-Temperature Metamorphism and S-type Granite Generation. *Lithos* 308-309, 168–180. doi:10.1016/j.lithos.2018.03.004
- Xu, Y.-G., Chung, S.-L., Shao, H., and He, B. (2010). Silicic Magmas from the Emeishan Large Igneous Province, Southwest China: Petrogenesis and Their Link with the End-Guadalupian Biological Crisis. *Lithos* 119 (1-2), 47–60. doi:10.1016/j.lithos.2010.04.013
- Xu, Y.-G., He, B., Chung, S.-L., Menzies, M. A., and Frey, F. A. (2004). Geologic, Geochemical, and Geophysical Consequences of Plume Involvement in the Emeishan Flood-Basalt Province. *Geology* 32 (10), 917–920. doi:10.1130/G20602.1
- Xu, Y.-G., Luo, Z.-Y., Huang, X.-L., He, B., Xiao, L., Xie, L.-W., et al. (2008). Zircon U-Pb and Hf Isotope Constraints on Crustal Melting Associated with the Emeishan Mantle Plume. *Geochimica Cosmochimica Acta* 72 (13), 3084–3104. doi:10.1016/j.gca.2008.04.019
- Xu, Y. G., Chung, S. L., Jahn, B. M., and Wu, G. Y. (2001). Petrologic and Geochemical Constraints on the Petrogenesis of Permian-Triassic Emeishan Flood Basalts in Southwestern China. *Lithos* 58 (3), 145–168. doi:10.1016/S0024-4937(01)00055-X
- Yan, Q., Metcalfe, I., and Shi, X. (2017). U-pb Isotope Geochronology and Geochemistry of Granites from Hainan Island (Northern South China Sea Margin): Constraints on Late Paleozoic-Mesozoic Tectonic Evolution. *Gondwana Res.* 49, 333–349. doi:10.1016/j.gr.2017.06.007
- Yunnan Geologic Bureau. (1973). *Geological Report of the Dali Area at Scale of 1: 200,000*. (in Chinese).
- Yunnan Geologic Bureau (1966). *Geological Report of the Heqing Area at Scale of 1: 200,000*. (in Chinese).

- Yan, Z., Tian, Y., Li, R., Vermeesch, P., Sun, X., Li, Y., et al. (2019). Late Triassic Tectonic Inversion in the Upper Yangtze Block: Insights from Detrital Zircon U-Pb Geochronology from South-Western Sichuan Basin. *Basin Res.* 31 (1), 92–113. doi:10.1111/bre.12310
- Yang, J., Cawood, P. A., Du, Y., Huang, H., and Hu, L. (2014). A Sedimentary Archive of Tectonic Switching from Emeishan Plume to Indosinian Orogenic Sources in SW China. *J. Geol. Soc.* 171 (2), 269–280. doi:10.1144/jgs2012-143
- Yang, J., Cawood, P. A., Du, Y., Huang, H., Huang, H., and Tao, P. (2012). Large Igneous Province and Magmatic Arc Sourced Permian-Triassic Volcanogenic Sediments in China. *Sediment. Geol.* 261–262, 120–131. doi:10.1016/j.sedgeo.2012.03.018
- Yang, J., Cawood, P. A., and Du, Y. (2015). Voluminous Silicic Eruptions during Late Permian Emeishan Igneous Province and Link to Climate Cooling. *Earth Planet. Sci. Lett.* 432 (1), 166–175. doi:10.1016/j.epsl.2015.09.050
- Yu, W., Algeo, T. J., Du, Y., Zhang, Q., and Liang, Y. (2016). Mixed Volcanogenic-Lithogenic Sources for Permian Bauxite Deposits in Southwestern Youjiang Basin, South China, and Their Metallogenic Significance. *Sediment. Geol.* 341, 276–288. doi:10.1016/j.sedgeo.2016.04.016
- Zhong, Y.-T., He, B., Mundil, R., and Xu, Y.-G. (2014). CA-TIMS Zircon U-Pb Dating of Felsic Ignimbrite from the Binchuan Section: Implications for the Termination Age of Emeishan Large Igneous Province. *Lithos* 204, 14–19. doi:10.1016/j.lithos.2014.03.005
- Zhong, Y.-T., He, B., and Xu, Y.-G. (2013). Mineralogy and Geochemistry of Claystones from the Guadalupian-Lopingian Boundary at Penglaitan, South China: Insights into the Pre-lopingian Geological Events. *J. Asian Earth Sci.* 62, 438–462. doi:10.1016/j.jseaes.2012.10.028
- Zhong, Y., Mundil, R., Chen, J., Yuan, D., Denyszyn, S. W., Jost, A. B., et al. (2020). Geochemical, Biostratigraphic, and High-Resolution Geochronological Constraints on the Waning Stage of Emeishan Large Igneous Province. *Geol. Soc. Am. Bull.* 132 (9–10), 1969–1986. doi:10.1130/B35464.1
- Zhou, M.-F., Zhao, J.-H., Qi, L., Su, W., and Hu, R. (2006). Zircon U-Pb Geochronology and Elemental and Sr-Nd Isotope Geochemistry of Permian Mafic Rocks in the Funing Area, SW China. *Contrib. Mineral. Pet.* 151 (1), 1–19. doi:10.1007/s00410-005-0030-y
- Zhou, M. F., Malpas, J., Song, X. Y., Robinson, P. T., Sun, M., Kennedy, A. K., et al. (2002). A Temporal Link between the Emeishan Large Igneous Province (SW China) and the End-Guadalupian Mass Extinction. *Earth Planet. Sci. Lett.* 196 (3), 113–122. doi:10.1016/S0012-821X(01)00608-2
- Zhou, Y. X., Wang, J., Zou, G. F., Wang, P., Ren, F., Dong, L. Y., et al. (2013). Study on Alluvial Fan-Delta Depositional System of Lower Triassic Qingtianbao Formation in Junmachang, Eryuan County, Western Yunnan. *Sediment. Geol. Tethyan Geol.* 33 (04), 6
- Zi, J.-W., Cawood, P. A., Fan, W.-M., Wang, Y.-J., Tohver, E., Mccuaig, T. C., et al. (2012). Triassic Collision in the Paleo-Tethys Ocean Constrained by Volcanic Activity in SW China. *Lithos* 144–145, 145–160. doi:10.1016/j.lithos.2012.04.020
- Zong, K., Klemm, R., Yuan, Y., He, Z., Guo, J., Shi, X., et al. (2017). The Assembly of Rodinia: The Correlation of Early Neoproterozoic (Ca. 900 Ma) High-Grade Metamorphism and Continental Arc Formation in the Southern Beishan Orogen, Southern Central Asian Orogenic Belt (CAOB). *Precambrian Res.* 290, 32–48. doi:10.1016/j.precamres.2016.12.010

Conflict of Interest: The authors declare that the research was conducted in the absence of any commercial or financial relationships that could be construed as a potential conflict of interest.

Publisher's Note: All claims expressed in this article are solely those of the authors and do not necessarily represent those of their affiliated organizations, or those of the publisher, the editors, and the reviewers. Any product that may be evaluated in this article, or claim that may be made by its manufacturer, is not guaranteed or endorsed by the publisher.

Copyright © 2022 Han, Huang, Yang, Wang and Luo. This is an open-access article distributed under the terms of the Creative Commons Attribution License (CC BY). The use, distribution or reproduction in other forums is permitted, provided the original author(s) and the copyright owner(s) are credited and that the original publication in this journal is cited, in accordance with accepted academic practice. No use, distribution or reproduction is permitted which does not comply with these terms.